Simulation of hydrogenated graphene field-effect transistors through a multiscale approach

G. Fiori*
Dipartimento di Ingegneria dell'Informazione: Elettronica, Informatica, Telecomunicazioni, Università di Pisa, Via Caruso 16, 56122 Pisa, Italy

S. Lebègue
Laboratoire de Cristallographie, Résonance Magnétique et Modélisations, CRM2, UMR CNRS 7036, Institut Jean Barriol, Nancy Université, BP 239, Boulevard des Aiguillettes, 54506 Vandoeuvre-lès-Nancy, France

A. Betti
Dipartimento di Ingegneria dell'Informazione: Elettronica, Informatica, Telecomunicazioni, Università di Pisa, Via Caruso 16, 56122 Pisa, Italy

P. Michetti
Institute for Theoretical Physics and Astrophysics, University of Wuerzburg, D-97074 Wuerzburg, Germany

M. Klintenberg and O. Eriksson
Department of Physics and Astronomy, Uppsala University, P.O. Box 516, SE-75120 Uppsala, Sweden

G. Iannaccone
Dipartimento di Ingegneria dell'Informazione: Elettronica, Informatica, Telecomunicazioni, Università di Pisa, Via Caruso 16, 56122 Pisa, Italy
and Smart Energy-Efficient Design (SEED) Center, Università di Pisa, Via dei Pensieri 60, 57128 Livorno, Italy

(Received 20 August 2010; published 7 October 2010)

In this work, we present a performance analysis of field-effect transistors (FETs) based on recently fabricated 100% hydrogenated graphene (the so-called graphane) and theoretically predicted semihydrogenated graphene (i.e., graphone). The approach is based on accurate calculations of the energy bands by means of GW approximation, subsequently fitted with a three-nearest neighbor sp^3 tight-binding Hamiltonian, and finally used to compute ballistic transport in transistors based on functionalized graphene. Due to the large energy gap, the proposed devices have many of the advantages provided by one-dimensional graphene nanoribbon FETs, such as large I_{on} and I_{on}/I_{off} ratios, reduced band-to-band tunneling, without the corresponding disadvantages in terms of prohibitive lithography and patterning requirements for circuit integration.

DOI: 10.1103/PhysRevB.82.153404 PACS number(s): 73.63.−b, 71.15.Mb, 72.80.Vp, 73.23.Ad

Chemical functionalization is a viable route toward band-gap engineering of graphene-based materials, as first demonstrated in Ref. 1, where exposure to a stream of hydrogen atoms has led to 100% hydrogenation of a graphene sheet, the so-called *graphane*. Obviously, research on functionalized graphene devices is at an embryonic stage. Several issues must be addressed to introduce graphane in future generations of electron devices. From this perspective, theoretical simulations can be very useful to explore possible solutions for device fabrication and design, in order to provide an early assessment of the opportunities of functionalized graphene in nanoscale electronics.

Sofo *et al.*[2] first predicted stability of 100% hydrogenated graphene through standard density-functional theory (DFT) calculations with a generalized gradient approximation (GGA). As also observed in Ref. 2, the H atom adsorption leads to sp^3 hybridization, where three of the sp^3 bonds are saturated by C atoms, and the fourth by H atom, which in turn induces an energy gap opening of few electron volts. More detailed simulations have been performed in Ref. 3, where DFT deficiencies in calculating energy gap have been overcome through GW simulations, showing energy gaps of 5.4 eV and 4.9 eV for the chair and the boat conformation, respectively, thus correcting results in Refs. 2 and 4 by almost 2 eV. Nonideal structures have been studied in Ref. 5, through geometry optimization and molecular-dynamics simulations. It has been shown that H frustration is very likely to occur, leading to extensive membrane corrugation, but also that hydrogenated domains, once formed, are very stable. Atomistic simulations have demonstrated that semihydrogenated graphene (*graphone*) with H atoms on the same side, possesses ferromagnetic properties, opening graphene to spintronic applications.[6]

Ferroelectric behavior has also been determined in Ref. 7, where "nanoroads" (i.e., graphene nanoribbons) have been defined on fully hydrogenated carbon sheets, exhibiting the same energy-gap behavior as a function of width as in Ref. 8. Gap opening can be induced not only through H functionalization but also by means of other absorbants.[9] Fluorine has been taken into account in Ref. 10, demonstrating a clear dependence of the energy gap on fluorine concentration, as well as lithium,[11] which however presents a geometrical conformation different from that in graphane, in which C atoms are pulled out by absorbants.

All mentioned articles are concerned with simulations of material properties, whereas studies on the operation and

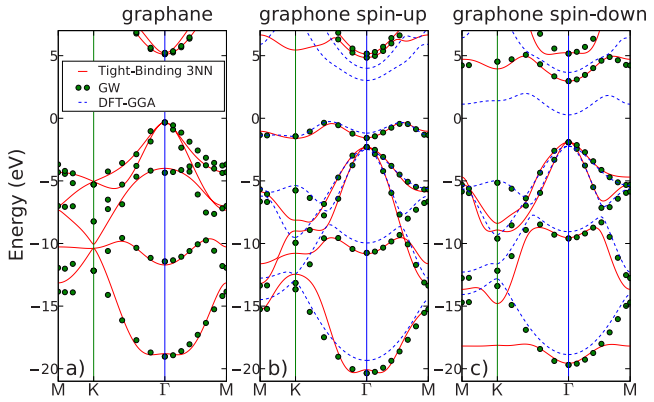

FIG. 1. (Color online) Energy bands computed for (a) graphane and [(b) and (c)] graphone, using tight-binding three-nearest neighbor (solid line), GW (dots), and DFT-GGA approaches (dashed lines). In the case of (b) graphone spin-up and (c) spin-down bands are shown.

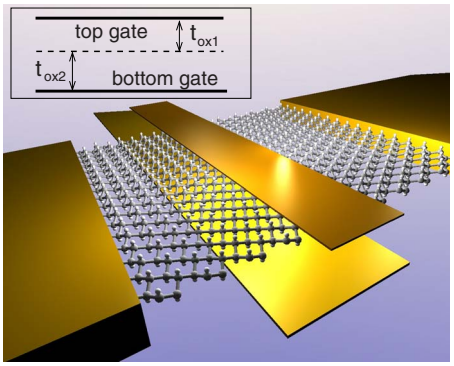

FIG. 2. (Color online) Sketch of the simulated device. The channel here shown is graphane but the very same structure has been considered for graphone based FET. In the inset, the device transversal cross section is shown.

performance of functionalized graphene-based devices are lacking, except for one work on current-voltage characteristics of graphane *p-n* junctions,[12] based on the effective mass approximation. Clearly, more efforts have to be directed toward this direction since whether graphane is suitable as a channel for field effect transistors is still an open issue, which can benefit from a contribution based on accurate numerical simulations.[13]

In order to address all these issues and to advance research in graphane electronics, we present a multiscale approach, based on (i) accurate GW calculations of the energy dispersion relations, (ii) a fitting of the computed energy bands by means of a three-nearest neighbor sp^3 tight-binding Hamiltonian to be included in a (iii) a semiclassical model, based on the assumption of ballistic transport, to simulate field-effect transistors based on graphane and graphone channels. In the context of this letter, we consider the best possible case and evaluate the achievable device performance. To this purpose, simple assumptions are useful: ballistic transport, regular hydrogenation, ohmic contacts, and ideal geometry. Certainly, manufacturability of the contacts and mobility require further investigation in wide gap channels, which is out of the scope of the present work.

In Fig. 1, we show the computed energy bands by means of three different models: three-nearest neighbor sp^3 tight-binding Hamiltonian (solid line), DFT within GGA of Perdew Burke Ernzerhof[14] (dashed line) and GW (dots).[15,16] DFT calculations have been performed by means of the Vienna *ab initio* simulation package,[17,18] which implements density functional theory[19,20] in the framework of the projector-augmented waves method.[21] Due to the presence of an unpaired electron in graphone,[6] we have allowed for spin polarization in all our calculations. In addition, since a ferromagnetic arrangement of the magnetic moments gives the smallest total energy,[6] we have considered the simplest cell that can accommodate this magnetic order, composed by two carbon and one hydrogen atoms.

Since the GGA approach is not suitable to treat excited states and the band gap, which is usually underestimated by standard exchange-correlation functionals such as the LDA or GGA, we have adopted the GW approximation (GWA). In particular, we have exploited the GW approximation as implemented in the code VASP,[22] which provides similar results as those from an earlier implementation.[23] In order to help convergence, we have considered 200 bands for the corresponding summation in the calculation of the polarizability and the self-energy while we have used a cutoff of 150 eV for the size of the polarizability matrices.

Since a comparison between DFT-GGA and GW in graphane has been extensively investigated in a previous article by some authors of the present paper,[3] here we just summarize the main features of its electronic structure. In the chair conformation, which is the most stable,[2] the gap is direct and in correspondence of the Γ point, and the band gap is equal to 3.5 eV for the GGA, and 5.4 eV (Ref. 3) for the more precise GW approximation. In the same way, the transitions at the high-symmetry points M and K are increased when considering the GW: from 10.8 to 13.7 eV at the M point, and from 12.2 to 15.9 eV at the K point.[3] The GW band structure of graphane presented here is exactly equivalent to the one in Ref. 3 and it is used here as a support for the tight-binding fitting.

In Figs. 1(b) and 1(c), we show spin-up and spin-down energy bands computed by means of the three abovementioned models for the 50% functionalized graphene sheet (graphone). The valence-band maximum is located along the Γ-K high-symmetry line [Fig. 1(b)] and almost degenerate with the other maximum along the Γ-M direction. The conduction-band minimum is instead at the Γ point [Fig. 1(c)]. For both GW and GGA the gap is indirect. However, while GGA provide a band gap equal to 0.46 eV, the GWA provides a band gap equal to 3.2 eV. In addition to increasing the band gap, the GWA is also modifying the dispersion relation with respect to GGA.

In order to solve the electrostatic and the transport problems in functionalized graphene devices, we have adopted a semiclassical model similar to that in Ref. 24, able to compute the free charge density and the current, given the energy bands in the whole Brillouin zone (BZ). The choice for such a model is justified by the large energy gap obtained for both graphane and graphone, which strongly limits the band-to-band tunneling component, differently to what happens in

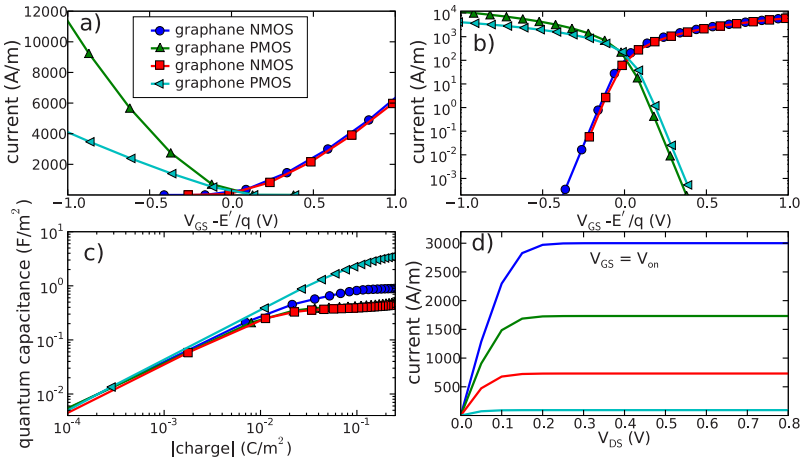

FIG. 3. (Color online) Transfer characteristics for graphane and graphone NMOS and PMOS in the (a) linear and in the (b) logarithmic scale: each transfer characteristic has been translated by E', the bottom of the conduction band for NMOS and the top of the valence band for PMOS; (c) quantum capacitance as a function of charge density in the channel; and (d) output characteristic for different V_{GS}: the gate-to-source step is 0.2 V.

carbon nanotubes,[25] graphene nanoribbon,[26] or graphene bilayer transistors.[27] The model relies on the assumption of fully ballistic transport since our aim in the current work is to assess the upper limits of device performance.

From a numerical point of view, a large number of k points in the BZ (almost equal to 10^5) is required in order to obtain accurate results, which can be really prohibitive for the GW approach. In order to avoid this problem, the energy dispersion along the ΓM and ΓK directions obtained by the GW approximation, has been fitted by means of a least-mean-square procedure and a three-nearest neighbor sp^3 tight-binding Hamiltonian, which has demonstrated to provide a better fitting as compared to a simple nearest-neighbor approach. Results are shown in Fig. 1. Particular attention has been paid to the minimum and the maximum of the conduction and valence bands, respectively, since such states are those mainly contributing to transport. As can be seen, tight-binding results are in good agreement with GW calculations.

In Fig. 2, we show the structure of the simulated double gate device. The channel is infinitely long and wide and embedded in SiO_2 (ε_r=3.9), which we consider a representative gate dielectric. Results can be translated to device with different gate dielectrics as long as the capacitance per unit area is the same. In the inset of Fig. 2, we show the device transversal cross section: t_{ox1} and t_{ox2} are the top and bottom gate oxide thicknesses, respectively.

In Figs. 3(a) and 3(b), the transfer characteristics of n-type metal-oxide semiconductor (NMOS) and p-type metal semiconductor (PMOS) FETs based on graphane and graphone are shown in the linear and logarithmic scale, for $t_{ox1}=t_{ox2}=1$ nm, and for a drain-to-source voltage $V_{DS}=V_{DD}=0.8$ V. To allow a comparison with the scaling expected for silicon technology, we consider the value of V_{DD} that the International Technology Roadmap for Semiconductors[28] predicts for high performance logic in 2015–2016. Analogously, the current in the OFF state I_{off} has been set to 100 nA/μm.

In the subthreshold regime, as expected, the subthreshold swing is equal to 60 mV/dec, due to the adopted double gate geometry, which assures good gate control over the channel barrier. As can be seen, all devices are able to provide large currents and almost present similar transfer characteristics as well as the same transconductance [derivative of the transfer characteristic with respect to gate-to-source voltage (V_{GS})], except for graphone PMOS, which shows degraded performance. This can be explained by its larger quantum capacitance (C_Q) [Fig. 3(c)], where C_Q for the four considered devices is depicted as a function of the charge density in correspondence of the channel. As can be seen, in the above threshold regime (charge density $>10^{-2}$ C/m^2), the graphone PMOS shows large C_Q, greater than the electrostatic capacitance ($C_{el}=6.9\times10^{-2}$ F/m^2).

From Fig. 3(c), one can also extract information concern-

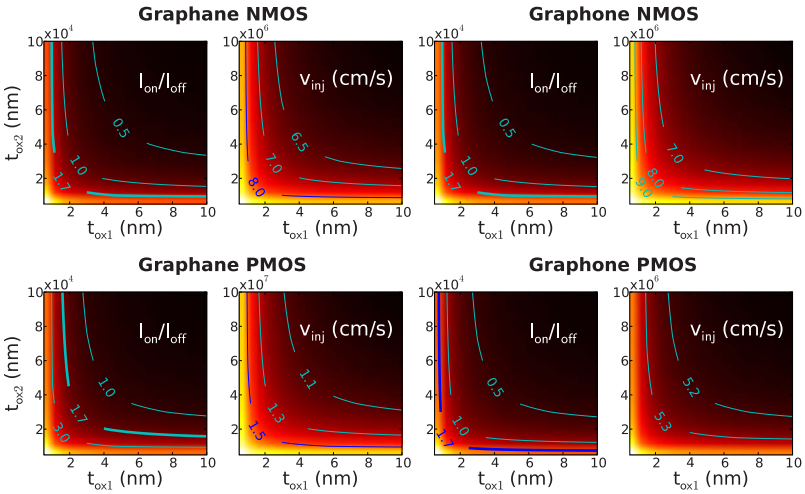

FIG. 4. (Color online) Color map of I_{on}/I_{off} ratios and injection velocity for graphane and graphone NMOS and PMOS devices as a function of t_{ox1} and t_{ox2}.

ing the effective mass. Quantum capacitance is indeed proportional in the flat region to the effective mass of the particle in the two-dimensional electron gas (2DEG).[29] As also confirmed by the curvature of the bands (which is inversely proportional to the effective mass), particles in graphone valence band are the heaviest ones. In Fig. 3(d) we show the drain-to-source current as a function of V_{DS}: the V_{GS} step is equal to 0.2 V.

Figure 4 shows the I_{on}/I_{off} ratio and the injection velocity for the four considered devices as a function of the top and bottom oxide thickness. Since I_{off} is fixed ($I_{off}=100$ nA/μm), I_{on} can be directly extracted from the color maps. The isolines for $I_{on}/I_{off}=1.7\times10^4$, which is the ratio required by the ITRS for the 2015–2016 technology, are also highlighted. As can be seen, all the devices manage to provide large ratios, even when considering top gate oxide thicknesses of almost 1 nm, and large bottom gate oxide thickness.

Injection velocity (v_{inj}) has been instead computed in correspondence of $V_{GS}=V_{on}$, defined as $V_{on}=V_{off}+V_{DD}$, where V_{off} is the V_{GS} at which the current is equal to I_{off} and represents the velocity of thermally emitted electrons from the reservoirs to the channel. Holes in graphone PMOS show the slowest velocity, in accordance with the above considerations, while the fastest particles are holes in graphane PMOS.

In conclusion, a multiscale approach has been adopted in order to assess potential of functionalized graphene as channel material for next-generation high-performance field-effect transistors. To achieve this task, calculations within the GW approximation have been performed in order to compute accurate energy bands and band gaps, which, in the case of graphone, has been demonstrated to differ by more than 2.7 eV from previous results. Tight-binding Hamiltonians for graphane and graphone have been fitted with GW results in order to feed a semiclassical model, able to compute transport in the whole Brillouin zone. Results have shown that graphane- and graphone-based FETs can provide large current as well as I_{on}/I_{off} ratios, and can represent a promising option for future technology nodes.

ACKNOWLEDGMENTS

The work was supported in part by the EC Seventh Framework Program under the Network of Excellence NANOSIL (Contract No. 216171), the STREP project GRAND (Contract No. 215752), and the MIUR-PRIN "Modeling and simulation of graphene nanoribbon FETs for high-performance and low-power logic applications" project (Prot. 2008S2CLJ9). S.L. acknowledges financial support from ANR PNANO under Grant No. ANR-06-NANO-053-02 and computer time using HPC resources from GENCI-CCRT/CINES (Grant No. 2010-085106). M.K. acknowledges financial support from the Swedish Research Council (VR), and the Göran Gustafsson Stiftelse. O.E. acknowledges VR and ERC for support.

*gfiori@mercurio.iet.unipi.it

[1] D. Elias, T. M. G. M. R. R. Nair, S. V. Morozov, P. Blake, M. P. Halsall, A. C. Ferrari, D. W. Boukhvalov, M. I. Katsnelson, A. Geim, and K. S. Novoselov, Science **323**, 610 (2009).
[2] J. O. Sofo, A. S. Chaudhari, and G. D. Barber, Phys. Rev. B **75**, 153401 (2007).
[3] S. Lebègue, M. Klintenberg, O. Eriksson, and M. I. Katsnelson, Phys. Rev. B **79**, 245117 (2009).
[4] J. Nakamura, N. Arimura, M. Hirayama, and A. Natori, Appl. Phys. Lett. **94**, 223107 (2009).
[5] M. Flores, P. Autreto, S. Legoas, and D. Galvao, Nanotechnology **20**, 465704 (2009).
[6] J. Zhou, Q. Wang, Q. Sun, X. S. Chen, Y. Kawazoe, and P. Jena, Nano Lett. **9**, 3867 (2009).
[7] A. K. Singh and B. I. Yakobson, Nano Lett. **9**, 1540 (2009).
[8] Y. W. Son, M. L. Cohen, and S. G. Louie, Phys. Rev. Lett. **97**, 216803 (2006).
[9] M. Klintenberg, S. Lebègue, M. I. Katsnelson, and O. Eriksson, Phys. Rev. B **81**, 085433 (2010).
[10] N. Lu, Z. Li, and J. Yang, J. Phys. Chem. C **113**, 16741 (2009).
[11] C.-K. Yang, Appl. Phys. Lett. **94**, 163115 (2009).
[12] B. Gharekhanlou and S. Khorasani, IEEE Trans. Electron Devices **57**, 209 (2010).
[13] G. Iannaccone, G. Fiori, M. Macucci, P. Michetti, M. Cheli, A. Betti, and P. Marconcini, Tech. Dig. - Int. Electron Devices Meet. **2009**, 245.
[14] J. P. Perdew, K. Burke, and M. Ernzerhof, Phys. Rev. Lett. **77**, 3865 (1996).
[15] L. Hedin, Phys. Rev. **139**, A796 (1965).
[16] L. Hedin and S. Lundquist, Solid State Phys. **23**, 1 (1969).
[17] G. Kresse and J. Furthmüller, Phys. Rev. B **54**, 11169 (1996).
[18] G. Kresse and D. Joubert, Phys. Rev. B **59**, 1758 (1999).
[19] P. Hohenberg and W. Kohn, Phys. Rev. **136**, B864 (1964).
[20] W. Kohn and L. Sham, Phys. Rev. **140**, A1133 (1965).
[21] P. E. Blöchl, Phys. Rev. B **50**, 17953 (1994).
[22] M. Shishkin and G. Kresse, Phys. Rev. B **74**, 035101 (2006).
[23] S. Lebègue, B. Arnaud, M. Alouani, and P. E. Bloechl, Phys. Rev. B **67**, 155208 (2003).
[24] S. Koswatta, N. Neophytou, D. Kienle, G. Fiori, and M. Lundstrom, IEEE Trans. Nanotechnol. **5**, 368 (2006).
[25] G. Fiori, G. Iannaccone, and G. Klimeck, IEEE Trans. Electron Devices **53**, 1782 (2006).
[26] G. Fiori and G. Iannaccone, IEEE Electron Device Lett. **28**, 760 (2007).
[27] G. Fiori and G. Iannaccone, IEEE Electron Device Lett. **30**, 261 (2009).
[28] http://www.itrs.net/Links/2009ITRS/Home2009.html
[29] S. Luryi, Appl. Phys. Lett. **52**, 501 (1988).